THE JOURNAL OF PHYSICAL CHEMISTRY B

Article

pubs.acs.org/JPCB

Combined Measurement of Translational and Rotational Diffusion in Quaternary Acyclic Ammonium and Cyclic Pyrrolidinium Ionic Liquids

Todd M. Alam,*[,†] Daniel R. Dreyer,[‡] Christopher W. Bielawski,[‡] and Rodney S. Ruoff[§]

[†]Department of Electronic and Nanostructured Materials, Sandia National Laboratories, Albuquerque, New Mexico 87185-0886, United States

[‡]Department of Chemistry and Biochemistry, The University of Texas at Austin, One University Station, A1590, Austin, Texas 78712, United States

[§]Department of Mechanical Engineering and the Materials Science and Engineering Program, The University of Texas at Austin, One University Station, C2200, Austin, Texas 78712, United States

Supporting Information

ABSTRACT: The translational self-diffusion coefficients (D_T) for a series of tetra-alkyl acyclic ammonium and cyclic pyrrolidinium ionic liquids (ILs) were measured using ^{1}H pulse field gradient (PFG) NMR spectroscopy over various temperatures. These NMR diffusion results were combined with previously measured rotational diffusion coefficients (D_R) obtained from ^{14}N NMR relaxation measurements for the same ILs (Alam, T. M.; et al. *J. Phys. Chem. A* **2011**, *115*, 4307−4316). The D_T/D_R ratio was then used to estimate the effective hydrodynamic radius and corresponding volumes without the need to directly measure the viscosities of the ILs. The generality, validity, and performance of using this D_T/D_R ratio is discussed and compared to the effective hydrodynamic volumes obtained using classic D_T/viscosity and D_R/viscosity relationships. The temperature variation observed for the molecular volumes obtained using the D_T/D_R ratio is argued to be a signature for the breakdown or decoupling of the Stokes−Einstein and Stoke−Einstein−Debye relationships in these neat IL systems, consistent with recent molecular dynamic simulations.

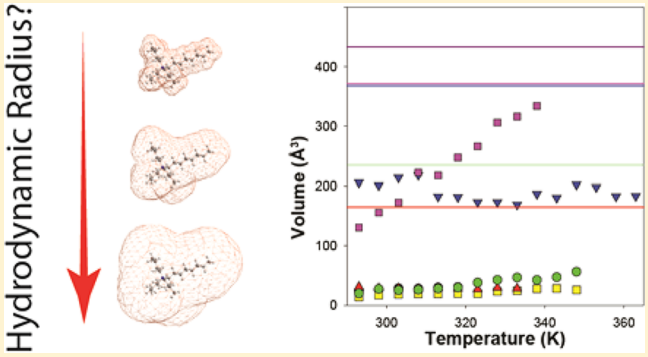

INTRODUCTION

Ionic liquids (ILs) continue to be incorporated into a wide range of applications including liquid electrolytes for energy storage and production devices, use in CO_2 capture, and as green solvents.[1−5] Understanding the transport properties as well as the ionic and solvent interactions of ILs is important for predicting their physicochemical properties.[6,7] The impact of structure, molecular organization, and cation/anion interactions on the physical properties of ILs is still not fully understood.[8] For example, the validity of the classic liquids description of molecular motions has been questioned when attempting to describe the transport properties of ILs. The Stokes−Einstein (SE) and Stokes−Einstein−Debye (SED) relationships connect the translational diffusion coefficient (D_T) or the rotational diffusion correlation times (τ_c) and rotational diffusion coefficient (D_R) to viscosity, temperature, and molecular volume. In a series of molecular dynamic (MD) simulations, deviations from the predicted SE and SED behaviors were observed for neat ILs and were attributed to dynamic heterogeneities present within these materials.[9]

A hallmark of dynamic heterogeneities is the breakdown of the SE relationship, which has been observed in supercooled liquids or fragile liquids near their glass transition temperatures (T_g).[10−14] Course-grain dynamic simulations also suggested that dynamic heterogeneity with nonexponential structural relaxation can lead to the violation of the SE relationship.[15] These violations have been described as the translational−rotation paradox,[16,17] decoupling of D_T and τ_c from viscosity,[12,18] or deviations from the SE and SED relationships.[19] The SE and SED breakdown is most commonly attributed to dynamic heterogeneities, but other studies in supercooled liquids attribute the observed behavior to a generalized breakdown of the classic SE and SED relationships.[20] Recent experimental results suggest that in ILs, these heterogeneities may exist and that deviations from the SE (D_T),[21] and SED (D_R)[22−24] relationships should be expected. However, the following questions remain: (1) How are dynamic motions to be described in ILs if dynamic heterogeneities are important for these systems and (2) how generalized are these observations for different ILs?

Received: November 12, 2012
Revised: January 15, 2013
Published: January 17, 2013

   dx.doi.org/10.1021/jp3111953 | *J. Phys. Chem. B* 2013, 117, 1967−1977

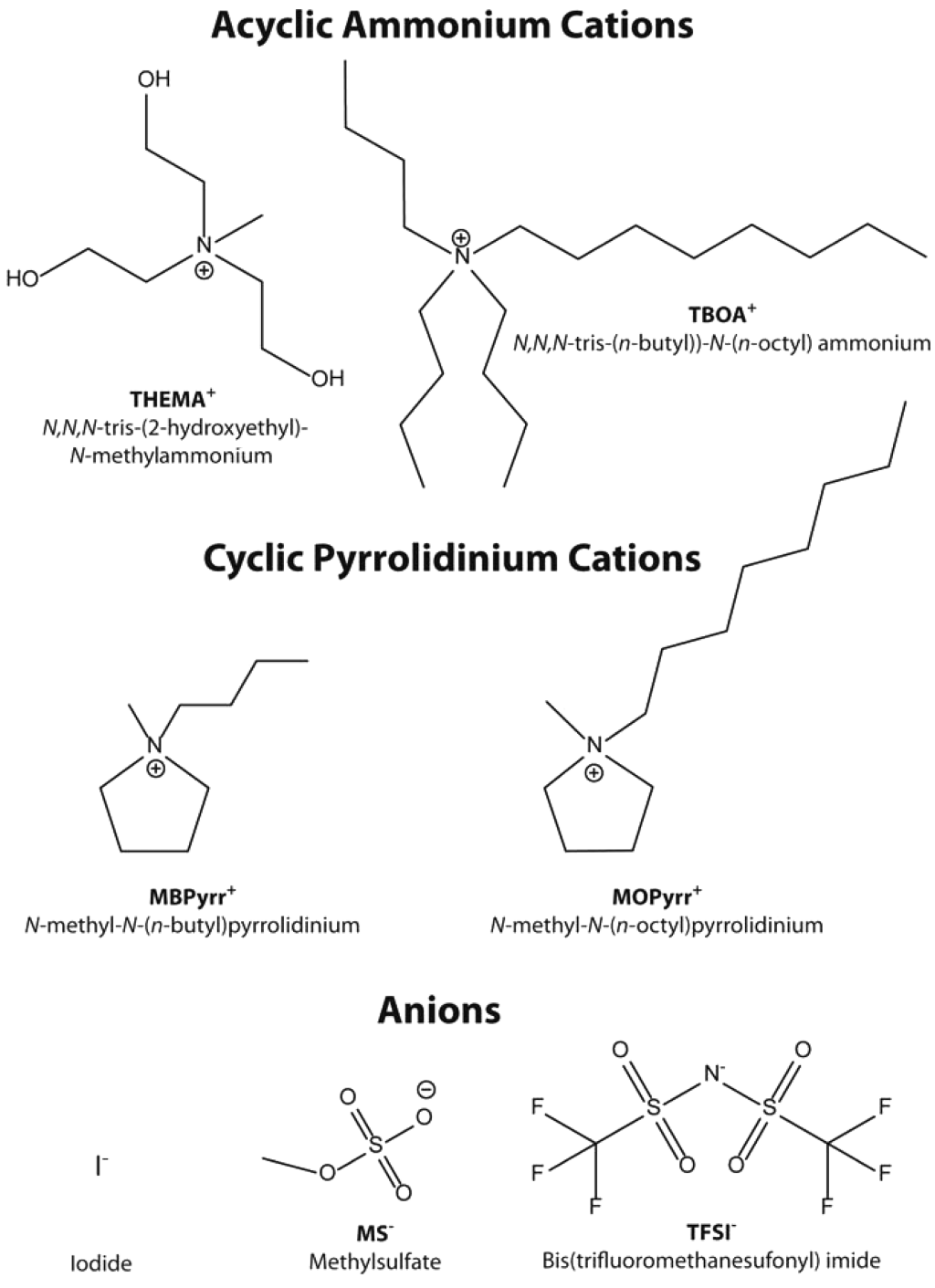

Figure 1. Various quaternary acyclic ammonium and cyclic pyrrolidinium cations with the selected anions for the ILs investigated.

NMR spectroscopy has proven to be an important tool for investigating the dynamics and transport properties of ILs. In particular pulse field gradient (PFG) NMR experiments allow the D_T's of both the cation and anion species to be directly measured. There have been multiple studies in ILs attempting to understand the factors controlling the structure[25,26] and electrochemical conductivity,[27−34] along with the role of water[35] and nanoconfinement in ILs.[36,37] Herein, we present ^{1}H PFG NMR diffusion data for a series of ILs containing quaternary ammonium and pyrrolidinium cations. In addition, these D_T results were combined with previous measurements of D_R obtained via ^{14}N NMR relaxation[38] in order to evaluate the effective hydrodynamic volumes and the performance of the SE and SED relationships.

EXPERIMENTAL SECTION

General Considerations. The ILs studied include *N,N,N*-tri-(*n*-butyl)-*N*-(*n*-octyl)ammonium bis-(trifluoromethanesulfonyl)imide ([TBOA]$^+$TFSI$^-$), *N,N,N*-tri-(*n*-butyl)-*N*-(*n*-octyl)ammonium methylsulfate ([TBOA]$^+$MS$^-$), *N*-methyl-*N*-(*n*-octyl)pyrrolidinium bis-(trifluoromethanesulfonyl)imide ([MOPyrr]$^+$TFSI$^-$), *N*-methyl-*N*-(*n*-octyl)pyrrolidinium methylsulfate ([MOPyrr]$^+$MS$^-$), *N*-methyl-*N*-(*n*-butyl)pyrrolidinium bis-(trifluoromethanesulfonyl)imide ([MBPyrr]$^+$TFSI$^-$), *N,N,N*-

dx.doi.org/10.1021/jp3111953 | J. Phys. Chem. B 2013, 117, 1967−1977

tris-(2-hydroxyethyl)-*N*-methylammonium iodide ([THEMA]$^+$I$^-$), and *N,N,N-tris*-(2-hydroxyethyl)-*N*-methylammonium methylsulfate ([THEMA]$^+$MS$^-$). The chemical structures of the investigated ILs are shown in Figure 1. The synthetic details for these materials have been previously reported,[38] while [MBPyrr]$^+$TFSI$^-$ was obtained directly from Aldrich. To reduce the impact of residual water, all ILs were sealed in 5 mm NMR tubes prior to storage and analysis, with the same sealed sample being used for both the ^{14}N NMR relaxation experiments[38] and the current ^{1}H PFG NMR diffusion analysis. While the water concentrations were not explicitly measured for these samples, the synthetic protocol attempted to keep water levels as low as possible. As a benchmark, ammonium ILs containing hydrophobic fluorinated anions prepared with similar heating and vacuum protocols typically have trace water levels below 50 ppm,[39] cyclic ammonium salts containing iodine anions were found to have water levels <250 ppm,[40] while Aldrich reports <200 ppm water levels for their commercial [MBPyrr]$^+$TFSI$^-$. In contrast, [THEMA]$^+$-based ILs are known to be hydroscopic, especially the MS$^-$ version, with water contents as high as 1900 ppm (0.19 wt %) being reported,[41] unless careful synthetic controls are employed.

NMR Measurements. The ^{1}H PFG NMR diffusion experiments were performed on a Bruker Avance-III instrument using a DIFF30 (30 A) *z*-gradient 5 mm diffusion probe. A bipolar stimulated echo pulse sequence was employed,[42] with the self-diffusion coefficients (D_T) determined from the signal decay using the classic Stejkal and Tanner equation[43] (eq 1)

$$S(g) = S(0)\exp\left[-D_T\gamma^2 g^2\delta^2\left(\Delta - \frac{\delta}{3}\right)\right] \quad (1)$$

where $S(g)$ and $S(0)$ are the integrated signal intensities obtained with and without gradients, respectively, D_T is the translational self-diffusion coefficient, γ is the gyromagnetic ratio, g is the gradient strength, δ is the duration of the gradient pulse, and Δ is the diffusion time delay between the gradient pulses. Typical experimental conditions included signal averaging with 8 scans, 16 gradient steps, a total gradient pulse length of δ = 1 ms, and a 5 s recycle delay. An interpulse delay (Δ) of 10 ms was used to reduce convection artifacts, with the gradient strength (maximum strength of 1300 G/cm) being adjusted to produce >90% signal reduction during the diffusion experiment. Only a single-exponential decay was observed for these PFG diffusion experiments, demonstrating that large polydispersity in the diffusion rate was absent.

The experimental details and analysis of the ^{14}N NMR experiments have previously been described.[38] In summary, the longitudinal spin−lattice ($R_1 = 1/T_1$) and transverse spin−spin ($R_2 = 1/T_2$) relaxation rates (which are the inverse of the relaxation times T_1 and T_2, respectively) were obtained using an inversion recovery and a CPMG (Carr−Purcell−Meiboom−Gill) pulse sequence and then combined to extract the rotational correlation time (τ_c) for each IL studied. For motions just outside of the extreme-motional limit, it was possible to obtain a unique solution to τ_c without knowledge of the ^{14}N quadrupolar coupling constant.

Association Energies and Molecular Volumes. Optimized structures for the associated cation and anion cluster along with the optimized structures for the isolated cations and anions in the gas phase were obtained using the 6-311++G(2d,2p) basis set,[44,45] density functional theory (DFT) utilizing Becke's three-parameter exchange functional,[46] and the LYP correlation function (B3LYP),[47] as implemented in Gaussian 09 software (Gaussian Inc., Wallingford, CT).[48] Initial starting structures for the associated ion pairs (IPs) were obtained using an initial molecular mechanics (MM) annealing prior to cluster optimization in Gaussian. In some instances, intermediate optimized structures were obtained at lower theory levels and provided the input for the final 6-311++G(2d,2p) basis set optimization. These optimized IP clusters are shown in Figure S1 (Supporting Information). There are a variety of methods to determine the molecular volume based on optimized ab initio structures. In this article, we report predicted volumes based on the SCF electron density (as implemented in Gaussian), which are expected to correlate simply with experimentally derived volumes (X-ray). These ab-initio-predicted volumes were compared to the volumes estimated from the combined NMR data.

The energies for association for the different IPs were defined using eq 2

$$\Delta E_{assoc} = E(\mathrm{IP}) - E(+) - E(-) \quad (2)$$

The first term, E(IP), is the total energy of the gas-phase optimized IP complex, while the next two terms are energies of the isolated and nonrelaxed (nonoptimized) cation and anion molecules. No corrections to the energy due to the basis set superposition error (BSSE) were evaluated but are expected to be relatively small in comparison to ΔE_{assoc}. Using eq 2, ΔE_{ads} < 0 values correspond to an exothermic association process. Similarly, it is possible to define an adsorption energy based on optimized cationic and anionic species using eq 3

$$\Delta E^{opt}_{assoc} = E(\mathrm{IP}) - E^{opt}(+) - E^{opt}(-) \quad (3)$$

where $E^{opt}(+)$ and $E^{opt}(-)$ are the energies for isolated and gas-phase optimized cation and anion structures, respectively. The difference between ΔE_{assoc} and ΔE^{opt}_{assoc} represent the energy for molecular deformations during complex formations.

Theoretical Background. The SE relationship is given by eq 4

$$D_T = \frac{k_B T}{6\pi\eta\xi_T r_{eff}} \quad (4)$$

where D_T is the translational diffusion coefficient, k_B is the Boltzmann constant, T is the temperature, η is the microviscosity, r_{eff} is the effective hydrodynamic radius of the molecule, and ξ_T is a scaling factor taking into account the slip/stick boundary condition, molecular size, and nonspherical molecular shape. Similarly, the NMR rotational correlations (τ_c) can be related to macroscopic properties using the SED relationship (eq 5)

$$\tau_c = \frac{\eta\xi_R V_{eff}}{k_B T} + \tau_0 = \frac{4\pi\eta\xi_R r^3_{eff}}{3k_B T} + \tau_0 \quad (5)$$

where V_{eff} is the effective molecular volume and ξ_R is the scaling factor for rotational motion. The offset factor τ_0 is related to the free rotor correlation times or the cross-correlation function between kinetic and torque-like terms.[49,50] This factor will commonly be dropped in evaluation of later approximations. Numerous scaling factors have been forwarded to estimate ξ_T and ξ_R[51] and will be discussed in the Results section.

Defining the rotational diffusion coefficient as $D_R = 1/6\tau_c$, the SED relationship (eq 5) reduces to eq 6

dx.doi.org/10.1021/jp3111953 | J. Phys. Chem. B 2013, 117, 1967−1977

$$D_R = \frac{k_B T}{8\pi\eta\xi_R r_{eff}^3} + \frac{1}{6k_B T\tau_0} \approx \frac{k_B T}{8\pi\eta\xi_R r_{eff}^3} \quad (6)$$

These SE and SED relationships can also be combined to provide an estimate of r_{eff} (eq 7)

$$\tau_c = \frac{2r_{eff}^2}{9D_T} + \tau_0 \quad (7)$$

or expressed in terms of the molecule radius or cluster radius (eq 8)

$$r_{eff} = \sqrt{\frac{9}{2}D_T(\tau_c - \tau_0)\frac{\xi_D}{\xi_R}} \approx \sqrt{\frac{9}{2}D_T\tau_c\frac{\xi_D}{\xi_R}} \quad (8)$$

For equivalent scaling factors (or scaling of unity), this relationship reduces to $r_{eff} = (4.5D_T\tau_c)^{1/2}$ and has been used in the description of supercooled liquids.[19,20] Introducing the definition of D_R reduces eq 8 to eq 9

$$r_{eff} = \sqrt{\frac{3D_T\xi_T}{4D_R\xi_R}} \quad (9)$$

This D_T/D_R ratio provides a way of estimating the effective molecular radius without the need to directly measure the local microviscosity of the ILs. Note that there is no explicit temperature dependence expected for this ratio.

RESULTS

Translational Self-Diffusion Coefficients. The translational self-diffusion coefficients were determined using ^{1}H PFG NMR spectroscopy for the ammonium and pyrrolidinium cations between 298 and 363 K; the data are shown in Figure 2.

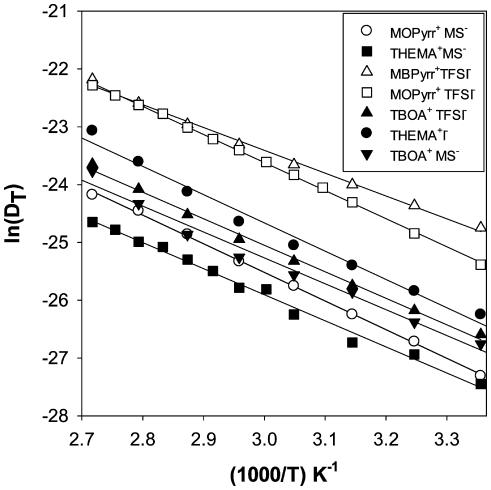

Figure 2. The variation of the translational diffusion coefficient (D_T) as a function of inverse temperature measured using ^{1}H PFG NMR spectroscopy for acyclic ammonium and cyclic pyrrolidinium ILs. An approximate Arrhenius behavior was observed for all systems over this temperature range.

While the diffusion rates for many ILs follow a Vogel–Tamman–Fulcher (VTF) behavior, a linear Arrhenius temperature behavior was observed for the current ILs over the limited temperature range investigated and was fit assuming (eq 10)

$$D_T(T) = D_0 \exp\left\{\frac{E_a}{RT}\right\} \quad (10)$$

The activation energies (E_a) and D_T at room temperature (298 K) are given in Table 1. The observed trend for $D_{T,298\ K}$ was $[MBPyrr]^+TFSI^-$ > $[MOPyrr]^+TFSI^-$ > $[THEMA]^+I^-$ > $[TBOA]^+TFSI^-$ > $[TBOA]^+MS^-$ > $[MOPyrr]^+MS^-$ > $[THEMA]^+MS^-$. This experimental trend does not correlate with the predicted molecular van der Waal (VDW) volumes (Table 2) of either the cation, V_{VDW}^{cation}, or the cation–anion IP, V_{VDW}^{IP}. As such, the result demonstrates that the structure and chemistry of both the cation and anion are important factors in determining the observed diffusion rate, and it is not simply the molecular size controlling the observed diffusion rates, although there are instances when simple volume estimates do provide a predictor (e.g., when only a single anion type is considered). In the $TFSI^-$ anion containing ILs, the trend in $D_{T,298\ K}$was $[MBPyrr]^+TFSI^-$ > $[MOPyrr]^+TFSI^-$ > $[TBOA]^+TFSI^-$; this trend was consistent with that predicted by the VDW volumes. In contrast, the ILs containing MS^- anions revealed the following trend for $D_{T,298\ K}$, $[TBOA]^+MS^-$ > $[MOPyrr]^+MS^-$ ≈ $[THEMA]^+MS^-$, which was the reverse order of the predicted cation volumes. In this case, there is both a change in the composition (e.g., the presence of hydroxyl groups in the $[THEMA]^+$) and a change in the molecular shape and polarity (i.e., cyclic versus acyclic).

Rotational Diffusion Rates. The rotational correlation times (τ_c) for the molecular reorientation for the aforementioned IL series have previously been determined by combining ^{14}N NMR spin–spin relaxation (R_2) and spin–lattice relaxation (R_1) measurements.[38] The temperature dependencies of τ_c for the different ILs are shown in Figure 3. (For additional experiment details and discussion on how τ_c was evaluated, the readers are directed to ref 38.) The room-temperature correlation time τ_c, the corresponding rotational diffusion rate, $D_R = (6\tau_c)^{-1}$, and the E_a are given in Table 1. It is important to note that the temperature range over which τ_c was determined is different for each IL and is smaller than the temperature range over which D_T was measured. This reduction in the temperature range investigated is due to the requirement that the ^{14}N NMR R_1 and R_2 relaxation rates must not be in the extreme narrowing limit in order to uniquely determine τ_c (without a prior knowledge of the quadrupolar coupling constant).[38] This limitation also prevented the estimation of τ_c for the rapidly tumbling $[MBPyrr]^+TFSI^-$ IL. The observed trend in $D_{R,298\ K}$ was $[THEMA]^+I^-$ > $[MOPyrr]^+TFSI^-$ > $[TBOA]^+TFSI^-$ > $[THEMA]^+MS^-$ > $[MOPyrr]^+MS^-$ > $[TBOA]^+MS^-$, which is very different than the trend observed for D_T. The E_a's determined from the D_T and D_R temperature variations are very similar, but the D_T derived values tend to be slightly larger. The exception was $[MOPyrr]^+TFSI^-$, which revealed a D_T activation energy that was approximately 10 kJ mol^{-1} larger than the E_a determined from D_R.

DISCUSSION

The translational self-diffusion results for the quaternary ammonium and cyclic pyrrolidinium ILs demonstrate that the molecular structure and chemistry of the cation–anion pair greatly impact the observed diffusional properties and are not simply explained by variations in molecular volume. For example, changing the anion can either produce no variation or an enhancement in D_T for a given cation, that is, compare the change in D_T between $[MOPyrr]^+MS^-$ and $[MOPyrr]^+TFSI^-$ to the invariant D_T measured for $[TBOA]^+MS^-$ and $[TBOA]^+TFSI^-$. Similarly, for a given anion, changes in the

dx.doi.org/10.1021/jp3111953 | J. Phys. Chem. B 2013, 117, 1967–1977

Table 1. Translational and Rotational Diffusion Coefficients, Correlation Times, and Activation Energies Obtained from Analysis of the ^{1}H PFG NMR Diffusion and ^{14}N NMR Relaxation Data and Glass Transition and Melting Temperatures for Various Quaternary Acyclic Ammonia and Cyclic Pyrrolidinium ILs

sample	D_T[a] (m^2 s^{-1})	E_a[b] (kJ mol^{-1}) [r^2]	τ_c (ns)	D_R[a] (s^{-1})	E_a[c] (kJ mol^{-1}) [r^2]	T_g[d] (K) [T_m]
[THEMA]$^+$I$^-$	3.4 ×10^{-12}	40.7 ± 1 [0.9840]	2.2	7.6 × 10^7	40.0 ± 0.4 [0.9994]	199.8[38]
[THEMA]$^+$MS$^-$	1.1 × 10^{-12}	37.5 ± 1 [0.9912]	5.0	3.3 × 10^7	36.3 ± 0.4 [0.9986]	226.6[38]
[TBOA]$^+$MS$^-$	2.2 × 10^{-12}	37.3 ± 1 [0.98152]	13.6	1.2 × 10^7	38.8 ± 0.4 [0.9971]	223.8[38]
[TBOA]$^+$TFSI$^-$	2.6 × 10^{-12}	38.1 ± [0.9955]	3.1	3.6 × 10^7	34.6 ± 0.3 [0.9991]	209.9[38]
[MBPyrr]$^+$TFSI$^-$	1.7 × 10^{-11}	32.9 ± 1 [0.9951] (29.3)[e]	–	–	29.2 ± 0.3 [0.9956]	190.1[27] [258.1][27] [255.1][67] [270.1][67] [267][68]
[MOPyrr]$^+$MS$^-$	1.4 × 10^{-12}	41.2 ± 1 [0.9991]	5.5	3.0 × 10^7	37.8 ± 0.4 [0.9924]	201.3[38]
[MOPyrr]$^+$TFSI$^-$	9.8 × 10^{-12}	40.4 ± 1 [0.9992]	2.5	6.6 × 10^7	28.9 ± 0.3 [0.9992]	231.0[38] 257.9[69]

[a]Evaluated at 298 K. [b]Energy of activation determined from the temperature dependence of ^{1}H PFG NMR diffusion rates, with the coefficient of determination r^2 given in brackets. [c]Energy of activation determined from the temperature dependence of ^{14}N R_2 relaxation rates. [d]Thermal glass transition or melting temperature and literature reference. [e]Evaluated from the diffusion data in ref 52.

Table 2. Experimental Molecular Volumes for Quaternary Acyclic Ammonia and Cyclic Pyrrolidinium ILs Obtained from the Analysis of the ^{1}H PFG NMR Diffusion and ^{14}N NMR Relaxation Data

sample	V_{eff} (Å^3) D_T/D_R[a]	V_{eff}^{GW} (Å^3) D_T/D_R[a,b]	V_{VDW}^{cation} (Å^3)[f]	V_{VDW}^{IP} (Å^3)[g]	ΔE_{assoc}[h] (kJ mol^{-1})	ΔE_{assoc}^{opt}[h] (kJ mol^{-1})
[THEMA]$^+$I$^-$	26.4	104	165	202	−386.9	−369.8
[THEMA]$^+$MS$^-$	17.2	68	165	230	−473.1	−420.0
[TBOA]$^+$MS$^-$	201.1	794	368	433	−316.0	−310.0
[TBOA]$^+$TFSI$^-$	28.6	113	368	505	−276.0	−270.5
[MBPyrr]$^+$TFSI$^-$	– [20.9][c] [33.0][c,d]	– [327] [516]	166	303	−302.6	−295.4
[MOPyrr]$^+$ MS$^-$	27.5 [5.1][c] [105.4][e]	108 [79.7] [659]	235	300	−346.2	−340.9
[MOPyrr]$^+$TFSI$^-$	155.7	613	235	372	−308.2	−300.6

[a]Evaluated using the D_T/D_R ratio (eq 9). [b]The Gierer-Wirtz (GW)-corrected volumes assume a scaling factor of ξ_R = 0.16, ξ_T = 0.4, and 0.633 for the D_T/D_R ratio in neat IL. [c]Evaluated from the variation of D_T with the temperature and inverse viscosity (Figure 4). [d]Estimated using D_T data from ref 52. [e]Evaluated from variation of $D_R = (6\tau_c)^{-1}$ as a function of temperature and inverse viscosity (Figure 4B). [f]Predicted van der Waals (VDW) volumes for the isolated cation using Gaussian 09. [g]Predicted VDW volumes for the cation−anion ion pair (IP). [h]Evaluated using eqs 2 and 3.

cation produce variations in D_T that do not always follow molecular size of shape arguments (Table 1). These results point to the difficulty of predicting the diffusion properties when there are major changes in the IL chemistry, size, or shape.

The temperature behavior of the self-diffusion has not been previously reported for the majority of these ILs; the exception is [MBPyrr]$^+$TFSI$^-$, where the D_T results reported here (Figure 2) are very similar to the temperature dependence study by Harris and Woolf[52] and are also consistent with the previous work of Tokuda and co-workers.[31] The magnitudes of D_T for the [MOPyrr]$^+$ and [MBPyrr]$^+$ cations are similar to previous results for the *N*-methyl-*N*-propyl pyrrolidinium [MPPyrr]$^+$ cation but show a dependence on the anion.[53] The observed activation energies (obtained from D_T) for [MOPyrr]$^+$MS$^-$ and [MOPyrr]$^+$TFSI$^-$ (~40−41 kJ mol^{-1}) are significantly larger than that that reported for [MPPyrr]$^+$TFSI$^-$ (~30.7 kJ mol^{-1}),[53] while the [MBPyrr]$^+$TFSI$^-$ activation energy (+32.9 kJ/mol) is very similar to the reported [MPPyrr]$^+$TFSI$^-$ value,[53] demonstrating that large changes in the chain length increase the translational diffusion activation energies.

The differences in the measured trends for the D_T and D_R hint at some of the difficulties in trying to describe the rotational and translational diffusion behavior in neat ILs. Inspection of the SE and SED relationships (eqs 4 and 5) argues that each is proportional to either $\xi_T r_{eff}$ or $\xi_R r_{eff}^3$ and that deviations from the trend based on the predicted van der Waals radius (or volume) behavior argue that either the scaling factors differ between rotational or translational motions or that the SE and SED relationships incompletely describe the dynamics of neat ILs. This idea will be further explored below.

Effective Molecular Volume Estimation Using Viscosity. The translational diffusion coefficients can be combined with viscosity measurements to estimate the effective volume using the SE relationship (eq 4). Figure 4 shows the variation of D_T versus k_BT/η for the [MBPyrr]$^+$TFSI$^-$ (Figure 4A) and

dx.doi.org/10.1021/jp3111953 | J. Phys. Chem. B 2013, 117, 1967−1977

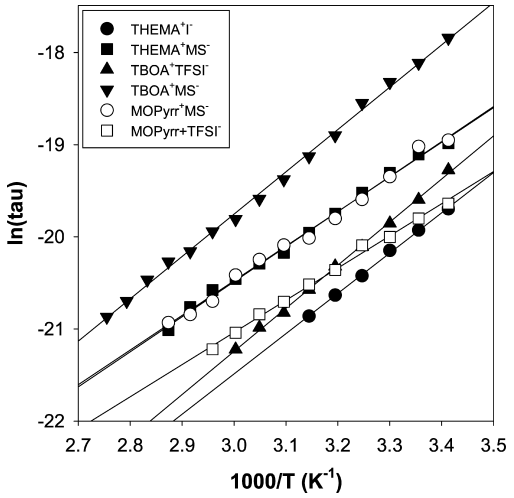

Figure 3. The variation of the rotational correlation time (τ_c) as a function of inverse temperature for acyclic ammonium and cyclic pyrrolidinium ILs. Correlation times measured using ^{14}N NMR relaxation experiments are described in ref 38.

[MOPyrr]$^+$TFSI$^-$ (Figure 4B). In addition, the diffusion data of Harris and Woolf for [MBPyrr]$^+$TFSI$^-$ over a slightly smaller temperature range are also analyzed (Figure 4A).[52] The viscosity data reported in the literature for the [MBPyrr]$^+$TFSI$^-$[52] and the extrapolated viscosity data of Salminen and co-workers for [MOPyrr]$^+$TFSI$^-$ were utilized.[54] These correlations predict V_{eff} values of 20.9 (current D_T data) and 33.0 Å^3 (Harris D_T data) for [MBPyrr]$^+$TFSI$^-$, along with a 5.1 Å^3 for [MOPyrr]$^+$TFSI$^-$. The estimated volumes are all significantly smaller than the predicted van der Waal volumes for the cations (V_{VDW}^{cation}) or the IPs (V_{VDW}^{IP}) shown in Table 2. Underestimation of the effective hydrodynamic volume is commonly encountered when analyzing diffusion and viscosity data and may result from the assumptions utilized. The classic SE and SED relationships assume a spherical molecule, which is clearly not appropriate for these molecules. It is also assumed that the molecule is diffusing in a viscous continuum solvent, which is also inappropriate for neat ILs. These issues have been addressed by the introduction of various scaling factors, which will be discussed below.

Similarly, the temperature/viscosity behavior of the rotational correlation time or the rotational diffusion coefficient (D_R) determined from ^{14}N NMR relaxation experiments can also be used to determine the molecular volume, as previously presented for the [MOPyrr]$^+$TFSI$^-$.[38] Figure 4B (open symbols) shows the variation of D_R versus k_BT/η evaluated using the SED relationship (eq 5). This correlation predicts an effective molecular volume of ~105 Å^3 (Table 2). Moreover, the predicted volume is larger than the 67 Å^3 previously reported for the same correlation time data set,[38] reflecting a slightly different extrapolation of the viscosity temperature data and the different weighting of data points in the linear fit using D_R instead of τ_c. Regardless, the predicted volume is significantly larger than the volume obtained from the D_T/viscosity data (~5 Å^3), again highlighting differences in the rotational and translational dynamics analyses. The D_R-estimated volume is smaller than the predicted V_{VDW}^{cation}.

The linear behavior observed between D_T or D_R and T/η (Figure 4) supports the general form of the SE and SED relationship and is approximately inversely linear to viscosity changes (η^{-1}). Linear SE behavior has been reported for several

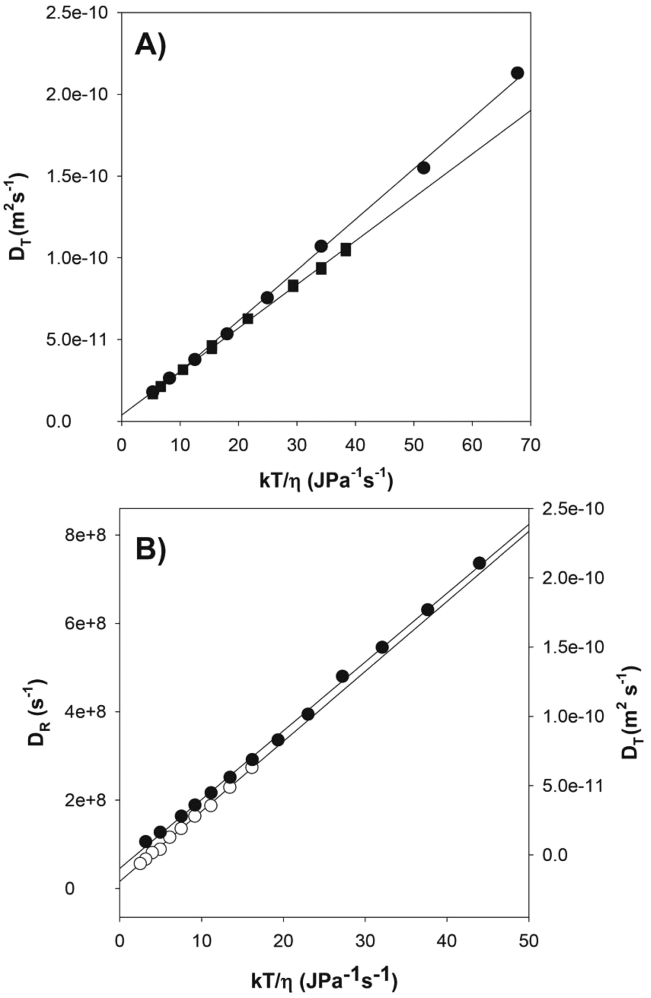

Figure 4. The variation of the translational diffusion coefficient D_T (● this study and ■ Harris and Woolf, ref 52) as a function of temperature and inverse shear viscosity for (A) [MBPyrr]$^+$TFSI$^-$ and (B) [MOPyrr]$^+$MS$^-$. The variation of the rotational diffusion coefficient D_R (○) for [MOPyrr]$^+$MS$^-$ is presented in (B). The straight lines represent fits to the Stokes–Einstein relationship for D_T (eq 4) and the Stokes–Einstein–Debye relationship for D_R (eq 5). These fits predict r_{eff} = 1.71 Å (D_T, this study) and 1.99 Å (ref 52) for [MBPyrr]$^+$TFSI$^-$ and r_{eff} = 2.93 Å (D_R) and 1.07 Å (D_T) for [MOPyrr]$^+$MS$^-$.

PFG NMR studies involving imidazolium- and pyridinium-based cations[32,33,53,55] and for thioether-functionalized ILs.[56] Yet, many of these PFG and relaxation NMR studies reveal experimental diffusion coefficients that are an order of magnitude faster than those predicted by the classic SE or SED equation.[32] On the other hand, modification to the relationships to take into account molecular shape and boundary conditions has been shown to produce corrected hydrodynamic volumes. For example, the ^{13}C NMR-based rotation correlation times in 1-ethyl-3-methylimidazoilium butanesulfonate[55] produce volumes that if scaled are similar to the predicted V_{VDW}^{cation}.

Effective Molecular Volume Estimation Using Combined Diffusion/Rotational Dynamics. The viscosity temperature dependence for the remaining ILs in this series was not available, precluding effective volume estimations using the viscosity correlations. Instead, the effective volumes were estimated using eqs 8 and 9, via the D_T/D_R ratio. In the limit of

dx.doi.org/10.1021/jp3111953 | J. Phys. Chem. B 2013, 117, 1967–1977

equivalent scaling factors, eq 9 reduces to $r_{eff} = (1/2)(3D_T/D_R)^{1/2}$. Using this limiting assumption, the estimated molecular volumes as a function of temperature are shown in Figure 5,

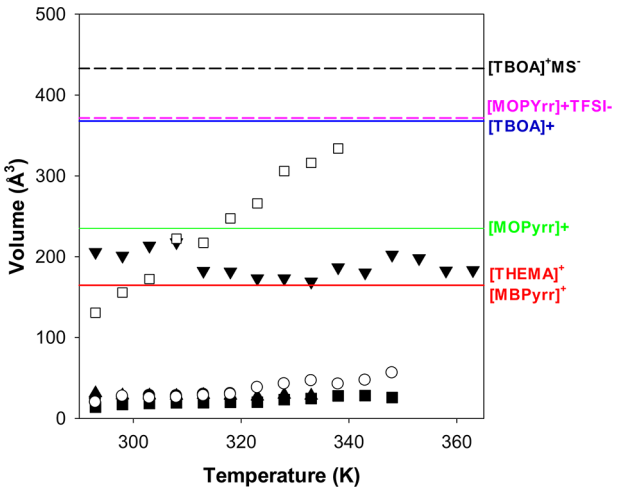

Figure 5. The variation of the effective molecular volume for the IL series obtained using the D_T/D_R ratio: $[THEMA]^+I^-$ (●), $[THEMA]^+MS^-$ (■), $[TBOA]^+MS^-$ (▼), $[TBOA]^+TFSI^-$ (▲), $[MOPyrr]^+MS^-$ (○), and $[MOPyrr]^+TFSI^-$ (□). The predicted van der Waal volumes for the cations (solid lines) and select IPs (dotted lines) are shown. See also Table 2.

with the 298 K volumes given in Table 2. There is not a volume for $[MBPyrr]^+TFSI^-$ reported using this method because the rotational correlation times were not determined for this IL.[38] This analysis reveals three different subclasses or behaviors in this series of ILs. Four of the ILs, $[THEMA]^+I^-$, $[THEMA]^+MS^-$, $[TBOA]^+TFSI^-$, and $[MOPyrr]^+MS^-$, have predicted molecular volumes within the ~15−30 Å^3 range and are consistent with the molecular volumes predicted for $[MBPyrr]^+TFSI^-$ using the D_T/viscosity correlations (Figure 4). The predicted volume for $[MOPyrr]^+MS^-$ using this method (27.5 Å^3) falls between the volumes predicted using the D_T/viscosity (5.1 Å^3) and the D_R/viscosity correlation (105.4 Å^3), as might be expected when using the D_T/D_R ratio for volume estimation. While these predicted volumes are still smaller than the van der Waal volumes, the introduction of appropriate scaling (see below) gives volumes that approach V_{VDW}^{cation}. The predicted volumes for these four ILs become slightly larger with increasing temperature, but overall, the temperature variation is relatively small (Figure 5). The $[TBOA]^+MS^-$ IL showed a different type of behavior, with a relatively large predictive volume of ~200 Å^3, which is smaller than V_{VDW}^{cation}, with the volume being about 10 times larger than the predicted volumes of the first four ILs. The volumes predicted for this IL shows very little temperature variation. The final type of behavior is demonstrated by $[MOPyrr]^+TFSI^-$, with a strong temperature variation in the predicted volumes, ranging from ~150 to 350 Å^3. This strong temperature dependence would be expected given the large differences in E_a obtained from D_T versus D_R data (Table 1). Differences in the association energies of the different cation−anion pairs were explored to determine if IP formation might explain the three different types of volume−temperature behavior. As a first approximation, the gas-phase association energies (ΔE_{assoc} and ΔE_{assoc}^{opt}) are given in Table 2 and range from −270 to −437 kJ/mol^{-1}, and are the same magnitude as that reported for other ILs.[57,58] The larger volumes predicted by $[TBOA]^+MS^-$ and $[MOPyrr]^+TFSI^-$ in comparison to those of the remaining ILs do not correlate with ΔE_{assoc} as there are several other IPs with similar values. Similarly, the strong temperature dependence of $[MOPyrr]^+TFSI^-$ does not correlate with the predicted ΔE_{assoc}. These reported association energies are for IPs in the gas phase, but it is understood that dielectric effects from the surrounding IL (or solvent) and ionic density profiles will impact the energies;[59] still, the relative trends in association energies are expected to remain similar. Water impurities are also known to play a significant role in affecting the physical properties of ILs and might explain these different types of volume−temperature behaviors. While the water content was not explicitly measured, it is suggested that the largest water concentrations would occur for ILs containing either the hydroxylated $[THEMA]^+$ cation or the MS^- anion. The strong observed temperature dependence of $[MOPyrr]^+TFSI^-$ would be argued not to be a result of water impurities due to the strong hydrophobic nature of the fluorinated $TFSI^-$ anion. Finally, we have assumed similar ξ_T and ξ_R scaling factors in estimating the effective hydrodynamic radius (eq 9). It may be that this assumption does not hold for all ILs or that scaling factors have temperature dependence (see the discussion below). An understanding of the causes giving rise to these different behaviors is unfortunately not clear but suggests that care must be taken when trying to compare diffusional or rotational dynamics for widely different ILs.

Combining of D_T and D_R has previously been used to estimate the effective hydrodynamic ratio for the cation in the quaternary ammonium IL [*N*,*N*-diethyl-*N*-methyl-*N*-(2-methoxyehtyl) ammonium] $TFSI^-$.[60] That study predicted an extremely small radius (0.9 Å), which was only ~25% of the predicted van der Waals radius (3.51 Å). This discrepancy was attributed to the use of the $^1H-^{13}C$ contribution for determining the molecular reorientation correlations time, with the possibility that local side-chain motions contributed to the dipolar relaxation measured by the ^{13}C T_1 and that the measured correlation time was a combination of these side-chain motions and the overall molecular reorientation. One of the benefits of the results presented in this paper is that the ^{14}N NMR R_1/R_2 relaxation is dominated by the molecular reorientation, particularly for the quaternary ammonium ILs, with limited dipolar contributions. For the pyrrolidinium ILs, there is the possibility of pseudo-rotation[61] of the ring leading to fluctuations in the ^{14}N electrical field gradient, but presently, the magnitude of these contributions on the ^{14}N relaxation have not been evaluated. Increases in the D_T/D_R ratio have also been observed in the MD simulations of $TFSI^-$ and bis(fluorosulfonyl)imide $(FSI)^-$-based ILs and were used as an indicator of differences in the temperature dependence of translational and rotational relaxation.[62]

Microviscosity Scaling Factors. Various models and approximations have been proposed to correct the microvisosity for different molecular shapes and boundary conditions. For example, Giere-Wirtz (GW) proposed a distance-dependent viscous friction for rotational dynamics that results in a correction factor (ξ_R) given by

$$\xi_R = \left[6\left(\frac{r_m}{r}\right) + \left(1 + \left(\frac{r_m}{r}\right)\right)^{-3}\right]^{-1} \quad (11)$$

where the ratio of the solvent molecule radius (r_m) and the solute IL cation (r) radius are the variables. For a neat IL (r_m =

dx.doi.org/10.1021/jp3111953 | J. Phys. Chem. B 2013, 117, 1967−1977

r), this reduces to $\xi_R = 0.16$. Similarly, the correction to the microviscosity for translational diffusion (ξ_T) is described by eq 11

$$\xi_T = \left(2\frac{r_m}{r} + \frac{1}{1 + r_m/r}\right)^{-1} \quad (12)$$

which reduced to 0.4 for the neat IL. In eq 9, the $(\xi_T/\xi_R)^{1/2}$ ratio introduces a 1.58 scaling factor to the predicted radius or a 3.95 factor to the predicted volume. The GW-corrected volumes using these scaling factors are given in Table 2. Other models have been proposed, including nonspherical molecular shapes under stick/slip boundary conditions,[63,64] and produce a range of correction factors. The magnitudes of these corrections are all similar to the GW scaling factors, leading to the same overall conclusions, and will not be pursued in detail here. These corrections bring the predicted volumes closer to V_{VDW}^{cation} for the majority of the IL series and, considering the numerous approximations, produce reasonable volumes. Unfortunately, the trends predicted by the VDW radius are not reflected in the experimental results. The $[TBOA]^+MS^-$ and $[MOPyrr]^+TFSI^-$ ILs have distinct behavior, with the introduction of these scaling factors predicting volumes that are significantly larger than even the cation/anion ionic pair (Table 2). This might suggest that for these two ILs, scaling factors are not required or have a different functionality or that larger aggregates beyond the simple IP contribute to the observed dynamics.

Signature of Diffusion and Rotational Dynamic Decoupling. The enhancement of the diffusion rate or predictions of small hydrodynamic volumes when using the SE relationship has been noted before and has been used to question the validity of these classic relationships when discussing the dynamics of neat ILs. For example, previous diffusion studies of imiadazolium ILs and protic ILs (PILs) have shown that the experimentally measured diffusion rates are an order of magnitude faster than would be predicted using the SE equation and known molecular volumes and viscosity.[32] The enhancement of the observed translational diffusion coefficients is not solely limited to experiment. MD simulations of diffusion and molecular rotations in ILs have also been used to back-calculate molecular volumes using SE and SED relationships. These predicted hydrodynamic volumes are consistently too small in neat ILs and only approach the predicted molecular volumes for dilute IL solutions.[9] Even by incorporating GW corrections to the derived volumes, the predictions remain too small. These MD simulations have been put forward as a demonstration of the breakdown of the SE or SED relations and are argued to result from dynamical heterogeneities present within the ILs.

In addition, many deviations from the linear SE diffusion have been describe well by a fractional SE relationship of the form[65]

$$D_T \propto \left(\frac{T}{\eta}\right)^m \quad (13)$$

with m ranging from approximately linear ($m = 1$), $m = 0.93$ for $[MBPyrr]^+TFSI^-$,[52] to between $m = 1$ and 0.66 for imidazolium ILs[32] and $m = 0.69$ for a series of PILs.[21] In the case of the latter, Burrell and co-workers demonstrated that there were differences in the low and high magnetic field translational diffusion rates and that the deviations from classic SE behavior were attributed to dynamic heterogeneities (most likely arising from hydrogen bond heterogeneities) and the corresponding differences in spin−spin T_2 relaxation behavior within the PILs.[21] For the ILs described in this paper, fractional behavior was not observed.

Another signature for deviations from the classic hydrodynamic SE or SED relationships is the temperature variance of the predicted V_{eff}. From eqs 8 and 9, it is assumed that the hydrodynamic volume or radius is temperature-independent and does not vary. In the MD simulations of neat ILs where the SE and SED relationship are argued to break down, it was observed that the V_{eff} values become smaller with a reduction in temperature.[19] This temperature variation was observed for the predicted V_{eff} obtained for five of the six ILs using the D_T/D_R method (Figure 4), with the predicted volumes increasing with increasing temperature. If the classic SE and SED relationships are valid for neat ILs, then the effective molecular radius, or D_T/D_R ratio, should be invariant with temperature.[20] Experimentally, this temperature variation is extremely noticeable for $[MOPyrr]^+TFSI^-$, with a >200% volume increase upon going from 298 to 338 K. The only exception to the temperature variation of volume was $[TBOA]^+MS^-$, which was approximately constant over the temperature range. It should be noted that while we did not observe a distinct distribution in the signal decay during the PFG NMR (multiexponential decay), the measured D_T would be dominated by the fast components of the diffusion if fast/slow distributions were present.[66] The increasing V_{eff} with increasing temperature is similar to the trend observed for simulations of supercooled water.[20] We suggest that this temperature variation in the predicted V_{eff} obtained using the D_T/D_R ratio method is a signature for the breakdown of the SE and SED relationship.

CONCLUSIONS

The translational self-diffusion coefficients D_T have been reported for a series of tetra-alkyl acyclic ammonium and cyclic pyrrolidinium ILs measured using ^1H pulse field gradient (PFG) NMR spectroscopy as a function of temperature. Combining these translational diffusion results with previous rotational diffusion coefficients (D_R) allowed the estimation of the effective molecular volumes that were consistent with the estimated volumes using the more conventional D_T/viscosity and D_R/viscosity correlations. Both methods produced estimated volumes that were significantly smaller than the predicted van der Waal volumes and required the introduction of scaling factors based on boundary conditions, shape, and size to improve the result.

Overall, the combined D_T/D_R ratio method for molecular volume estimation provided consistent results for the majority of the ILs in the series studied but did reveal that some ILs have translational or rotational dynamics that result in the prediction of very large molecular volumes, without the need to provide scaling factors. These results suggest that care should be exercised when comparing volume estimates obtained from D_T or D_R for widely different ILs. The temperature variation in the predicted volumes based on the D_T/D_R ratio, most notably for the $[MOPyrr]^+TFSI^-$ IL, were argued to be evidence that there is decoupling of the SE and SED relationships and that a more completed description for translational and rotational dynamics in neat ILs needs to be developed.

dx.doi.org/10.1021/jp3111953 | J. Phys. Chem. B 2013, 117, 1967−1977

■ ASSOCIATED CONTENT

Supporting Information

The structures of the gas-phase optimized IL clusters investigated and the complete citations for refs 34, 48, and 61. This material is available free of charge via the Internet at http://pubs.acs.org.

■ AUTHOR INFORMATION

Corresponding Author

*Phone: (505) 844-1225. Fax: (505) 844-2974. E-mail: tmalam@sandia.gov.

Notes

The authors declare no competing financial interest.

■ ACKNOWLEDGMENTS

This research was funded by the U.S. DOE, Office of Basic Energy Sciences, under Award ER46657. Sandia National Laboratories is a multiprogram laboratory operated by Sandia Corporation, a wholly owned subsidiary of Lockheed Martin Company, for the U.S. Department of Energy's National Nuclear Security Administration under Contract DE-AC04-94AL85000.

■ REFERENCES

(1) Endres, F.; Zein El Abedin, S. Air and Water Stable Ionic Liquids in Physical Chemistry. *Phys. Chem. Chem. Phys.* **2006**, *8*, 2101−2116.

(2) Rogers, R. D.; Seddon, K. R. Ionic Liquids—Solvents of the Future? *Science* **2003**, *302*, 792−793.

(3) Wishart, J. F. Energy Applications of Ionic Liquids. *Energy Environ. Sci.* **2009**, *2*, 956−961.

(4) Kim, T. Y.; Lee, H. W.; Stoller, M. D.; Dreyer, D. R.; Bielawski, C. W.; Ruoff, R. S.; Suh, K. S. High-Performance Supercapacitors Based on Poly(Ionic Liquid)-Modified Graphene Electrodes. *ACS Nano* **2011**, *5*, 436−442.

(5) Karadas, F.; Atilhan, M.; Aparicio, S. Review on the Use of Ionic Liquids (ILs) as Alternative Fluids for CO_2 Capture and Natural Gas Sweetening. *Energy Fuels* **2010**, *24*, 5817−5828.

(6) Ueno, K.; Tokuda, H.; Watanabe, M. Ionicity in Ionic Liquids: Correlation with Ionic Structure and Physiochemical Properties. *Phys. Chem. Chem. Phys.* **2010**, *12*, 1649−1658.

(7) Chaban, V. V.; Voroshylova, J. V.; Kalugin, O. N.; Prezhdo, O. V. Acentonitrile Boosts Conductivity on Imidazolium Ionic Liquids. *J. Phys. Chem. B* **2012**, *116*, 7719−7727.

(8) Spohr, H. V.; Patey, G. N. Structural and Dynamical Properties of Ionic Liquids: Competing Influences on Molecular Properties. *J. Chem. Phys.* **2010**, *132*, 154504.

(9) Köddermann, T.; Ludwig, R.; Paschek, D. On the Validity of Stokes−Einstein and Stokes−Einstein−Debye Relations in Ionic Liquids and Ionic Liquid Mixtures. *ChemPhysChem* **2008**, *9*, 1851−1858.

(10) Ediger, M. D. Spatially Heterogeneous Dynamics in Supercooled Liquids. *Annu. Rev. Phys. Chem.* **2000**, *51*, 99−128.

(11) Jung, Y.; Garrahan, J. P.; Chandler, D. Excitation Lines and Breakdown of Stokes−Einstein Relations in Supercooled Liquids. *Phys. Rev. E: Stat., Nonlinear, Soft Matter Phys.* **2004**, *69*, 061205.

(12) Blackburn, F. R.; Cicerone, M. T.; Hietpas, G.; Wagner, P. A.; Ediger, M. D. Cooperative Motion in Fragile Liquids near the Glass Transition: Probe Reorientation in O-Terphenyl and Polystyrene. *J. Non-Cryst. Solids* **1994**, *172−174*, 256−264.

(13) Chang, I.; Sillescu, H. Heterogeneity at the Glass Transition: Translational and Rotational Self-Diffusion. *J. Phys. Chem. B* **1997**, *101*, 8794−8801.

(14) Eaves, J. D.; Reichman, D. R. Spatial Dimension and the Dynamics of Supercooled Liquids. *Proc. Natl. Acad. Sci. U.S.A.* **2009**, *106*, 15171−15175.

(15) Jeong, D.; Choi, M. Y.; Kim, H. J.; Jung, Y. Fragility, Stokes−Einstein Violation, and Correlated Local Excitations in a Coarse-Grained Model of an Ionic Liquid. *Phys. Chem. Chem. Phys.* **2010**, *12*, 2001−2010.

(16) Stillinger, F. H.; Hodgdon, J. A. Translation−Rotation Paradox for Diffusion in Fragile Glass-Forming Liquids. *Phys. Rev. E: Stat., Nonlinear, Soft Matter Phys.* **1994**, *50*, 2064−2068.

(17) Stillinger, F. H.; Hodgdon, J. A. Reply to "Comment on 'Translation−Rotation Paradox for Diffusion in Fragile Glass-Forming Liquids'". *Phys. Rev. E: Stat., Nonlinear, Soft Matter Phys.* **1996**, *53*, 2995−2997.

(18) Chang, I.; Fujara, F.; Geil, B.; Heuberger, G.; Mangel, T.; Sillescu, H. Translational and Rotational Molecular Motion in Supercooled Liquids Studied by NMR and Forced Rayleigh Scattering. *J. Non-Cryst. Solids* **1994**, *172−174* (Part 1), 248−255.

(19) Kind, R.; Liechti, O.; Korner, N.; Hulliger, J.; Dolinsek, J.; Blinc, R. Deuteron-Magnetic-Resonance Study of the Cluster Formation in the Liquid and Supercooled-Liquid State of 2-Cyclooctylamino-5-Nitropyridine. *Phys. Rev. B: Condens. Matter Mater. Phys.* **1992**, *45*, 7697−7703.

(20) Mazza, M. G.; Giovambattista, N.; Stanley, H. E.; Starr, F. W. Connection of Translational and Rotational Dynamical Heterogeneities with the Breakdown of Stokes−Einstein and Stokes−Einstein−Debye Relations in Water. *Phys. Rev. E: Stat., Nonlinear, Soft Matter Phys.* **2007**, *76*, 031203.

(21) Burrell, G. L.; Burgar, I. M.; Gong, Q.; Dunlop, N. F.; Separovic, F. NMR Relaxation and Self-Diffusion Study and High and Low Magnetic Fields of Ionic Association in Protic Ionic Liquids. *J. Phys. Chem. B* **2010**, *114*, 11436−11443.

(22) Schröder, C.; Wakai, C.; Weingärtner, H.; Steinhauser, O. Collective Rotational Dynamics in Ionic Liquids: A Computational and Experimental Study of 1-Butyl-3-Methyl-Imidazolium Tetrafluoroborate. *J. Chem. Phys.* **2007**, *126*, 084511.

(23) Daguenet, C.; Dyson, P. J.; Krossing, I.; Oleinikova, A.; Slattery, J.; Wakai, C.; Weingärtner, H. Dielectric Response of Imidazolium-Based Room-Temperature Ionic Liquids. *J. Phys. Chem. B* **2006**, *110*, 12682−12688.

(24) Antony, J. H.; Dölle, A.; Mertens, D.; Wasserscheid, P.; Carper, W. R.; Wahlbeck, P. G. ^{13}C NMR Relaxation Rates in the Ionic Liquid 1-Methyl-3-Nonylimidazolium Hexafluorophosphate. *J. Phys. Chem. A* **2005**, *109*, 6676−6682.

(25) Judeinstein, P.; Iojoiu, C.; Sanchez, J.-Y.; Ancian, B. Proton Conducting Ionic Liquid Organization as Probed by NMR: Self-Diffusion Coefficients and Heteronuclear Correlations. *J. Phys. Chem. B* **2008**, *112*, 3680−3683.

(26) Liao, C.; Shao, N.; Han, K. S.; Sun, X.-G.; Jiang, D.-E.; Hagaman, E. W.; Dai, S. Physicochemical Properties of Imidazolium-Derived Ionic Liquids with Different C-2 Substitutions. *Phys. Chem. Chem. Phys.* **2011**, *13*, 21503−21510.

(27) Tokuda, H.; Tsuzuki, S.; Susan, M. A. B. H.; Hayamizu, K.; Watanabe, M. How Ionic Are Room-Temperature Ionic Liquids? An Indicator of the Physicochemical Properties. *J. Phys. Chem. B.* **2006**, *110*, 19593−19600.

(28) Álvarez, V. H.; Dosil, N.; Gonzalez-Cabaleiro, R.; Mattedi, S.; Martin-Pastor, M.; Iglesias, M.; Navaza, J. M. Bronsted Ionic Liquids for Sustainable Processes: Synthesis and Physical Properties. *J. Chem. Eng. Data* **2010**, *55*, 625−632.

(29) Tokuda, H.; Hayamizu, K.; Ishii, K.; Susan, M. A. B. H.; Watanbe, M. Physicochemical Properties and Structures of Room Temperature Ionic Liquids. 1. Variation of Anionic Species. *J. Phys. Chem. B* **2004**, *108*, 16593−16600.

(30) Tokuda, H.; Hayamizu, K.; Ishii, K.; Susan, M. A. B. H.; Watanbe, M. Physicochemical Properties and Structures of Room Temperature Ionic Liquids. 2. Variation of Alkyl Chain Length in Imidazolium Cation. *J. Phys. Chem. B* **2005**, *2005*, 6103−6110.

(31) Tokuda, H.; Ishii, K.; Susan, M. A. B. H.; Tsuzuki, S.; Hayamizu, K.; Watanbe, M. Physicochemical Properties and Structures of Room-Temperature Ionic Liquids. 3. Variation of Cationic Structures. *J. Phys. Chem. B* **2006**, *110*, 2833−2839.

(32) Chung, S. H.; Lopato, R.; Greenbaum, S. G.; Shirota, H.; Castner, E. W., Jr.; Wishart, J. F. Nuclear Magnetic Resonance Study of the Dynamics in Imidazolium Ionic Liquids with $-CH_2Si(CH_3)_3$ Versus $CH_2C(CH_3)_3$ Substituents. *J. Phys. Chem. B.* **2007**, *111*, 4885−4893.
(33) Susan, M. A. B. H.; Noda, A.; Watanabe, M. In *Electrochemical Aspects of Ionic Liquids*; Ohno, H., Ed.; John Wiley & Sons, Inc.: New York, 2011; pp 65−85.
(34) Seki, S.; Hayamizu, K.; Tsuzuki, S.; Fujii, K.; Umebayahi, Y.; Mitsugi, T.; Kobayashi, T.; Ohno, Y.; Kobayashi, Y.; Mita, Y.; et al. Relationships between Center Atom Species (N, P) and Ionic Conductivity, Viscosity, Density, Self-Diffusion Coefficient of Quaternary Cation Room-Temperature Ionic Liquids. *Phys. Chem. Chem. Phys.* **2009**, *11*, 3509−3514.
(35) Menjoge, A.; Dixon, J.; Brennecke, J. F.; Maginn, E. J.; Vasenkov, S. Influence of Water on Diffusion in Imidazolium-Based Ionic Liquids: A Pulse Field Gradient NMR Study. *J. Phys. Chem. B* **2009**, *113*, 6353−6359.
(36) Iacob, C.; Sangoro, J. R.; Papdopoulos, P.; Schubert, T.; Naumov, S.; Valiullin, R.; Käregr, J.; Kremer, F. Charge Transport and Diffusion of Ionic Liquids in Nanoporous Silica Membranes. *Phys. Chem. Chem. Phys.* **2010**, *12*, 13798−13803.
(37) Iacob, C.; Sangoro, J. R.; Kipnusu, W. K.; Valiullin, R.; Kärger, J.; Kremer, F. Enhnaced Charge Transport in Nano-Confined Ionic Liquids. *Soft Matter* **2012**, *8*, 289−293.
(38) Alam, T. M.; Dreyer, D. R.; Bielwaski, C. W.; Ruoff, R. S. Measuring Molecular Dynamics and Activation Energies for Quaternary Acyclic Ammonium and Cyclic Pyrrolidinium Ionic Liquids Using ^{14}N NMR Spectroscopy. *J. Phys. Chem. A* **2011**, *115*, 4307−4316.
(39) Katase, T.; Imashuku, S.; Marase, K.; Hirato, T.; Awakura, Y. Water Content and Related Physical Properties of Aliphatic Quantenary Ammonium Imide-Type Ionic Liquid Containing Metal Ions. *Sci. Technol. Adv. Mater.* **2006**, *7*, 502−510.
(40) Sun, I.-W.; Wang, H. P.; Teng, H.; Su, S.-G.; Lin, Y.-C.; Kuo, C.-W.; Chen, P.-R.; Wu, T.-Y. Cyclic Ammonium-Based Ionic Liquids as Potential Electrolytes for Dye-Synthesized Solar Cells. *Int. J. Electrochem. Sci.* **2012**, *7*, 9748−9764.
(41) Aparicio, S.; Atilhan, M. Insights into Tris-(2-hydroxyethyl) Methylammonium Methylsulfate Aqueous Solutions. *ChemPhysChem* **2012**, *13*, 3340−3349.
(42) Cotts, R. M.; Hoch, M. J. R.; Sun, T.; Marker, J. T. Pulse Field Gradient Stimulated Echo Methods for Improved NMR Diffusion Measurements in Heterogeneous Systems. *J. Magn. Reson.* **1989**, *83*, 252−266.
(43) Stejskal, E. O.; Tanner, J. E. Spin Diffusion Measurements: Spin Echos in the Presence of a Time Dependent Field Gradient. *J. Chem. Phys.* **1965**, *42*, 288−292.
(44) McLean, A. D.; Chandler, G. S. Contracted Gaussian Basis Sets for Molecular Calculations. I. Second Row Atoms, Z = 11−18. *J. Chem. Phys.* **1980**, *72*, 5639−5648.
(45) Krishnan, R.; Binkley, J. S.; Pople, J. A. Self-Consistent Molecular Orbital Methods. XX. A Basis Set for Correlated Wave Functions. *J. Chem. Phys.* **1980**, *72*, 650−654.
(46) Becke, A. D. Density-Functional Thermochemistry. III. The Role of Exact Exchange. *J. Chem. Phys.* **1992**, *98*, 5648−5652.
(47) Lee, C.; Yang, W.; Parr, R. G. Development of the Colle−Salvetti Correlation-Energy Formula into a Functional of the Electron Density. *Phys. Rev. B* **1988**, *37*, 785−789.
(48) Frisch, M. J.; Trucks, G. W.; Schlegel, H. B.; Scuseria, G. E.; Robb, M. A.; Cheeseman, J. R.; Scalmani, G.; Barone, V.; Mennucci, B.; Petersson, G. A. et al. *Gaussian 09*; Gaussian, Inc.: Wallingford, CT, 2009.
(49) Evilla, R. F.; Robert, J. M.; Whittenburg, S. L. NMR Studies of Rotational Motion at Low Viscosity. *J. Phys. Chem.* **1989**, *93*, 6550−6552.
(50) Rudakoff, G.; Oehme, K.-L. The Slip-Model for Molecular Reorientation and the Temperature Dependence of Nuclear Relaxation Times in Neat Toluene and Chlorobenzene. *Chem. Phys. Lett.* **1978**, *54*, 342−346.
(51) Macchioni, A.; Ciancaleoni, G.; Zuccaccia, C.; Zuccacaccia, D. Determining Accurate Molecular Sizes in Solution through NMR Diffusion Spectroscopy. *Chem. Soc. Rev.* **2008**, *37*, 479−489.
(52) Harris, K. R.; Woolf, L. A. Transport Properties of *N*-Butyl-*N*-Methylpyrrolidinium Bis(Trifluoromethylsufonyl)Amide. *J. Chem. Eng. Data* **2011**, *56*, 4672−4685.
(53) Hayamizu, K.; Tsuzuki, S.; Seki, H.; Fujii, K.; Suenaga, M.; Umebayahi, Y. Studies of the Translational and Rotational Motions of Ionic Liquids of *N*-Methyl-*N*-propyl-pyrrolidinium (P_{13}) Cation and Bis(trifluuoromethanesufonyl) Amide and Bis(fluorosulfonyl) Amide Anions and Their Binary Systems Including Lithium Salts. *J. Chem. Phys.* **2010**, *133*, 194505.
(54) Saliminen, J.; Papaiconomou, N.; Kumar, R. A.; Lee, J.-M.; Kerr, J.; Newman, J.; Prausnitz, J. M. Physicochemical Properties and Toxicities of Hydrophobic Piperdinium and Pyrrolidinium Ionic Liquids. *Fluid Phase Equilib.* **2007**, *261*, 421−426.
(55) Heimer, N. E.; Wilkes, J. S.; Wahlbeck, P. G.; Carper, W. R. ^{13}C Nmr Relaxation Rates in Ionic Liquid 1-Ethyl-3-Methylimidazolium Butanesulfonate. *J. Phys. Chem. A* **2006**, *110*, 868−874.
(56) Torriero, A. A. J.; Siriwardana, A. I.; Bond, A. M.; Burgar, I. M.; Dunlop, N. F.; Deacon, G. B.; MacFarlane, D. R. Physical and Electrochemical Properties of Thiolether-Functionalized Ionic Liquids. *J. Phys. Chem. B* **2009**, *113*, 11222−11231.
(57) Lehmann, S. B. C.; Roatsch, M.; Schoppke, M.; Kirchner, B. On the Physical Origin of the Cation−Anion Intermediate Bond in Ionic Liquids Part I. Placing a (Weak) Hydrogen Bond between Two Charges. *Phys. Chem. Chem. Phys.* **2010**, *12*, 7473−7486.
(58) Thompson, D.; Coleman, S.; Diamond, D.; Byrne, R. Electronic Structure Calculations and Physicochemical Experiments Quantify the Competitive Liquid Ion Association and Probe Stabilisation Effects for Nitrobenzospiropyran in Phosphonium-Based Ionic Liquids. *Phys. Chem. Chem. Phys.* **2011**, *13*, 6156−6168.
(59) Maiti, A.; Rogers, R. D. A Correlation-Based Predictor for Pair-Association in Ionic Liquids. *Phys. Chem. Chem. Phys.* **2011**, *13*, 12138−12145.
(60) Hayamizu, K.; Tsuzuki, S.; Seki, S.; Ohno, Y.; Miyashiro, H.; Kobayashi, Y. Quaternary Ammonium Room-Temperature Ionic Liquid Including and Oxygen Atom in Side/Chain/Lithium Salt Binary Electrodes: Ionic Conductivitya and ^{1}H, ^{7}Li and ^{19}F NMR Studies of Diffusion Coefficients and Local Motions. *J. Phys. Chem. B* **2008**, *112*, 1189−1197.
(61) Umebayahi, Y.; Mitsugi, T.; Fujii, K.; Seki, S.; Chiba, K.; Yamamoto, H.; Lopes, J. N. C.; Padua, A. A. H.; Takeuchi, M.; Kanzaki, R.; et al. Raman Spectroscopic Study, DFT Calculations and MD Simulations on the Conformational Isomerism of *N*-Alkyl-*N*-Methylpyrrolidinium Bis-(trifluoromethanesufonyl) Amide Ionic Liquids. *J. Phys. Chem. B.* **2009**, *113*, 4338−4346.
(62) Borodin, O.; Gorecki, W.; Smith, G. D.; Armand, M. Molecular Dynamics Simulation and Pulsed-Field Gradient NMR Studies of Bis(fluorosulfonyl)imide (FSI) and Bis[(trifluoromethyl)sulfonyl]-Imide (TFSI)-Based Ionic Liquids. *J. Phys. Chem. B* **2010**, *114*, 6786−6798.
(63) Hu, C.-M.; Zwanzig, R. Rotational Friction Coefficients for Spheroids with the Slipping Boundry Conditions. *J. Chem. Phys.* **1974**, *60*, 4354−4357.
(64) Youngren, G. K.; Acrivos, A. Rotational Friction Coefficients for Ellipsoids and Chemical Molecules with the Slip Boundry Conditions. *J. Chem. Phys.* **1975**, *63*, 3846−3848.
(65) Becker, S. R.; Poole, P. H.; Starr, F. W. Fractional Stokes−Einstein and Debye−Stokes−Einstein Relations in a Network-Forming Liquid. *Phys. Rev. Lett.* **2006**, *97*, 055901.
(66) Sillescu, H. Heterogeneity at the Glass Transition: A Review. *J. Non-Cryst. Solids* **1999**, *243*, 81−108.
(67) Henderson, W. A.; Passerini, S. Phase Behavior of Ionic Liquid−LiX Mixtures: Pyrrolidinium Cations and $TFSI^-$ Anions. *Chem. Mater.* **2004**, *16*, 2881−2885.

(68) Kunze, M.; Montanino, M.; Appetecchi, G. B.; Jeong, S.; Schönhoff, M.; Winter, M.; Passerini, S. Melting Behavior and Ionic Conductivity in Hydrophobic Ionic Liquids. *J. Phys. Chem. A* **2010**, *114*, 1776−1782.
(69) Appetecchi, G. B.; Montanino, M.; Zane, D.; Carewska, M.; Alessandrini, F.; Passerini, S. Effect of the Alkyl Group on the Synthesis and the Electrochemical Properties of *N*-Alkyl-*N*-Methyl-Pyrrolidinium Bis(trifluoromethanesulfonyl)imide Ionic Liquids. *Electrochim. Acta* **2009**, *54*, 1325−1332.